THE ASTROPHYSICAL JOURNAL, 292:670–675, 1985 May 15

35 DAY SPECTROSCOPIC EFFECTS IN HZ HERCULIS

J. B. HUTCHINGS, E. M. GIBSON, D. CRAMPTON, AND W. A. FISHER
Dominion Astrophysical Observatory
Received 1984 September 19; accepted 1984 November 21

ABSTRACT

New spectroscopic data are presented of HZ Her, which have ~2 Å resolution, and cover both 1.7 day orbital and 35 day (precessional?) periods. Data include measures of principal absorption-line velocities and asymmetries, and emission-line velocities and intensities. Orbital parameters derived from Balmer and He I velocities are found to be modulated over half the 35 day period of the system. This can be generally understood in terms of a variable X-ray heating, modulated by a thick precessing disk about the secondary. Models for such a variable heating fit the principal effects and yield a primary star orbital velocity of 83 ± 3 km s^{-1}. This implies masses of 1.91 and 0.93 $M_\odot$ for the two stars. The emission-line features are found to vary in velocity with an amplitude of ~105 km s^{-1} and a phase shift of 0.3 with respect to the absorption, suggesting a principal origin above the trailing side of the heated face of the primary star. Line intensity variations are discussed and lend support to these conclusions.

Subject headings: stars: individual — X-rays: binaries

I. INTRODUCTION AND DATA

The binary system HZ Her is well known as the optical counterpart to the galactic X-ray source Her X-1 (see Bradt and McClintock 1983, and references therein). The system has a 1.7 day binary orbit, with a strong light modulation due to X-ray heating effects on the primary. There is also a 35 day cycle in X-ray intensity and light curve modulation, generally understood as precession of an optically thick accretion disk about the X-ray pulsar component of the binary. Much work has been published on the X-ray pulse timing and the X-ray and optical light curves (Gerend and Boynton 1976; Crosa and Boynton 1980; Deeter, Boynton, and Pravdo 1981; Gorecki *et al.* 1982; Howarth and Wilson 1983). Optical pulses have been detected by Middleditch and Nelson (1976) in the emission lines, suggesting that they arise on the heated sides of the optical primary. The optical spectroscopic orbit was studied by Crampton (1974) and Crampton and Hutchings (1974) (hereafter Papers I and II, respectively). Since that time, no further optical orbital studies have been made, in spite of improved detectors and spectral resolution. We have accumulated data with the DAO 1.8 m telescope, with improved resolution and signal to noise over the earlier work. Most of the data are spectrograms at 38 Å mm^{-1}, 0.8 mm wide, with the EMI three-stage image tube. Some data were obtained using an 1872 element Reticon detector behind the image tube. All spectrograms were measured for radial velocity on the ARCTURUS comparator, and ~30 of them, selected for quality and phase coverage, were converted into rectified intensity tracings using the interactive program REDUCE (Hill, Poeckert, and Fisher 1982). Reticon spectra were reduced using REDUCE. In Table 1 we show the new data and the principal measures made on them.

The radial velocity data comprise four main groups. These are the absorption features of H, He I, and Ca II, and the group of emission lines of N V, N III, and He II in the 4600–4700 Å range. The emission lines were measured as a complete group from spectrum tracings, using a template with the six principal lines. The individual emission lines were generally too weak and noisy to measure directly with ARCTURUS. The absorption-line data were grouped as mentioned because of the very strong differences in orbital phase dependence, discussed in Papers I and II. The quoted absorption-line velocities are all derived from the line cores. In the Balmer lines, definite asymmetries were found, so that the line core and wing velocities are sometimes significantly different. Weights are quoted for the measured quantities; these are a reflection of the overall quality of each spectrogram, the number of lines comprising the value quoted, and the scatter of measures from individual lines.

Equivalent widths were measured for the strongest lines of each ion, and an asymmetry measure was derived for the Hγ and Hδ lines. The asymmetry index is the ratio of the area of the absorption shortward of the line minimum to that longward. While weak blends and noise may cause systematic errors in these numbers, the good agreement between the asymmetry index for the two lines suggests that the changes are real and intrinsic to the Balmer lines.

Spectra were binned according to orbital phase, and the summed spectra for several phases are shown in Figure 1. These summed spectra are dominated by 1.7 day phase effects, and the 35 day effects discussed below are not obvious in the figure.

II. ORBITAL ANALYSIS

Orbital parameters were derived for the three groups of absorption lines, (*a*) using the new data alone, and (*b*) combined with the earlier data of Papers I and II. We adopted the period of 1.70016773 day derived by Deeter, Boynton, and Pravdo (1981) from the X-ray data, since our data cannot improve on it. The results given by the old and new sets of data were not significantly different—in fact they were very close—so that the full combined data set was used in all the radial velocity analysis which follows. As in Papers I and II, the three groups of lines were found to yield very different orbital parameters, including apparent phase shifts from the orbital determination from the X-ray pulse timing (see Table 2). The residuals from the orbital fits were then examined for dependence on the 35 day cycle of Her X-1. First, the residuals themselves were examined to look for modulation of the V_0 velocity. Second, the residuals were reversed for X-ray (1.7 day)

TABLE 1

HZ HERCULIS DATA AND MEASURES

HJD	PHASE[a]		RADIAL VELOCITIES (km.s^{-1})				EQUIV. WIDTHS (A)			ASYMMETRY[e]	
2,440,000+	$1^{d}.7$	35d	H I	He I	Ca II	Emis[b]	H[c]	He I[d]	Emis[b]	Hδ	Hγ
3328.797	0.897	0.295	-156±24	-	-	-	-	-	-	-	-
3365.737	0.624	0.353	-58±19	-	-	-	-	-	-	-	-
3371.745	0.158	0.525	5±14	-	-13	-	-	-	-	-	-
3372.737	0.741	0.553	-128±23	-	-181	-	-	-	-	-	-
3638.919	0.304	0.174	-11±19	-	67	-	-	-	-	-	-
3960.948	0.714	0.394	-98±26(2)	-	-145	65	5.4	0.88	2.6	0.77	0.67
3960.953	0.717	0.394	-125±27(3)	-	-152	-	5.3	-	2.3	1.08	1.10
3960.960	0.721	0.394	-116±39(2)	-	-	16(2)	4.7	0.75	2.5	1.08	0.83
3960.966	0.724	0.394	-112±12(3)	-125±25	-	180	4.9	0.67	1.7	0.70	0.73
3960.970	0.727	0.395	-120±34(2)	-87±22(2)	-	-75(2)	5.2	0.88	2.7	0.64	0.87
3960.976	0.730	0.395	-96±18(2)	-93	-	-75(2)	5.0	0.79	2.1	1.11	0.65
4014.792	0.384	0.936	1±6 (3)	-	-25	-40(2)	4.9	0.83	1.9	1.25	1.14
4014.795	0.386	0.936	-	-	-	-30(2)	4.9	0.71	1.6	1.00	1.00
4014.798	0.387	0.936	18±8	-	-	-30(2)	4.7	0.46	1.3	1.00	1.00
4014.801	0.389	0.936	-	-	-	-30(2)	4.6[f]	0.79	2.5	-	-
4014.803	0.390	0.936	-40±17	-10	-	-18(2)	5.0	0.88	1.8	1.44	1.18
4014.806	0.392	0.936	-	-	-	0(2)	4.8	0.88	-	1.33	1.00
4014.809	0.393	0.936	-21±8 (2)	6	-	-16(2)	4.1	0.83	1.6	1.83	0.93
4014.812	0.395	0.936	-	-	-	-30(2)	4.6	0.92	2.8	0.60	0.93
4015.814	0.985	0.965	-68±26(3)	-	-94	-	10.3	0.33	2.7	1.54	0.95
4015.826	0.991	0.965	-68±29(2)	-	-	-120(2)	12.1	0.58	2.0	1.73	0.76
4015.837	0.998	0.966	-23±48	-	-	-225(2)	10.9	0.67	2.2	1.57	0.70
4015.848	0.005	0.966	-55±50	-	-	-	-	-	-	-	-
4015.859	0.011	0.966	-49±41(2)	-	-	-	-	-	-	-	-
4015.869	0.017	0.967	-60±17(2)	-	-	-	-	-	-	-	-
4051.760	0.127	0.994	-67±10(2)	-	-57	-60	4.4	-	1.6	1.33	1.09
4052.746	0.707	0.022	-96±13(3)	-	-140	20(2)	5.1	0.79	1.1	1.20	1.00
4112.709	0.976	0.739	-50±14(2)	-	-	-	8.6	0.38	-	1.23	1.00
4112.719	0.982	0.740	-67±10(2)	-	-57	-	8.5	-	-	1.21	1.00
4112.730	0.988	0.740	-67±14(2)	-	-72	-225(2)	11.4	-	-	1.25	1.00
4755.821	0.240	0.152	-50±26(2)	-87	-	-75(2)	8.9	1.33	2.4	1.33	1.00
5113.816	0.805	0.401	-162±24(2)	-	-126	-	-	-	-	-	-
5113.859	0.830	0.402	-166±18	-	-	-	-	-	-	-	-
5119.787	0.317	0.572	-28±19(3)	-7(2)	-	-	-	-	-	-	-
5119.798	0.323	0.572	-35±13	-	-	-	-	-	-	-	-
5119.838	0.346	0.574	-38±15	-48	-	-	-	-	-	-	-
5135.847	0.762	0.032	-16±13(2)	-48±8(2)	-	-	-	-	-	-	-
5135.861	0.771	0.032	-18±11(2)	-50	-	-	-	-	-	-	-
5139.909	0.152	0.148	-6±10(2)	-	-	-	-	-	-	-	-
5140.778	0.663	0.173	-	-	-	-	5.2	0.33	0.6	1.38	1.30
5140.787	0.668	0.173	-89±15(3)	-	-	-	-	-	-	-	-
5141.749	0.234	0.201	-36±28(2)	-84	-	-150(2)	5.9[f]	1.00	1.3	1.00	-
5141.755	0.238	0.201	-	-	-	-90(2)	8.8[f]	1.00	1.0	1.42	-
5142.762	0.830	0.230	-105±26(2)	-	-	-60(2)	8.2	0.54	0.7	1.20	0.93
5143.761	0.418	0.259	-16±10(2)	-18±10(2)	-18	0(2)	6.3	1.04	1.8	1.50	0.93
5144.771	0.012	0.287	-87±31(2)	-	-66	-	-	-	-	-	-
5145.782	0.606	0.316	-70±17(3)	-86±17(2)	-62	-	-	-	-	-	-
5168.787	0.137	0.975	-	-	-	-165(2)	4.0	0.50	0.4	1.14	0.80
5172.740	0.462	0.088	21±16(2)	-13±6	8	-	-	-	-	-	-
5440.013	0.666	0.740	-55±8 (2)	-	-	30(2)	4.2[f]	0.46	0.6	1.10	-
5492.907	0.777	0.255	-124±27	-26	-	-75(2)	5.4	0.63	2.3	1.17	0.91
5493.902	0.362	0.283	13±17(2)	-	-	-	-	-	-	-	-
5534.763	0.396	0.453	-43±13	-70	-22	-	-	-	-	-	-
5534.776	0.404	0.453	-18±25(3)	-43±4(2)	-	-	-	-	-	-	-
5534.826	0.433	0.455	14±10(2)	-26	-	-	-	-	-	-	-

NOTE.—Numbers in parentheses are the associated weights other than 1.

[a] 2,441,329.57519 + 1.70016773E; 2,442,410.329 + 34.928E.

[b] Combined: N V λ4603, 19; N III λ4634, 40, 41; He II λ4686.

[c] Hδ and Hγ mean.

[d] He I λ4471 line.

[e] Ratio of blue wing to red wing.

[f] Only one line measured.

phases 0.5 to 1.0, and left unchanged for phases 0.0 to 0.5, in order to look for modulation of orbital velocity amplitude (e.g., a larger amplitude will produce opposite residuals during the approaching and receding parts of the orbit). Significant ($> 3\ \sigma$) modulations were found in the H and He I line data sets, folded on 35 and 17.5 day periods. Table 3 shows the relevant numbers. The modulations are larger on the 17.5 day cycle, and the apparent 35 day modulation is probably seen as a result of uneven data distribution. Furthermore, the 17.5 day result is easily compatible with the generally accepted precessing disk model, while the 35 day modulation is not. Power spectrum analysis of all the residual data sets did not reveal any other significant periodicity.

The orbital determinations were then repeated, with the radial velocity data binned in two sets of 35 day cycle phases. These yielded the other orbital parameter sets shown in Table

1985ApJ...292..670H

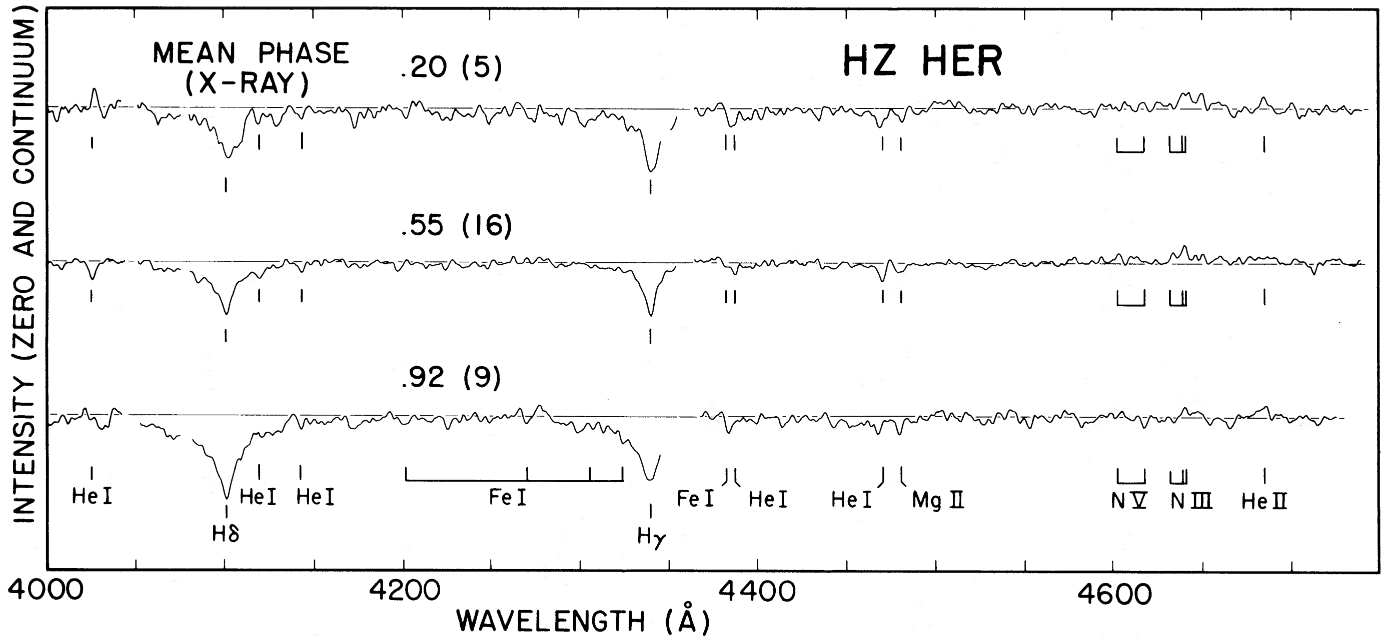

FIG. 1.—Averaged spectra of HZ Her in orbital phase bins. Mean phases are indicated, and in parentheses, the number of spectra averaged. Note the changes in Balmer and He I line strengths. Missing parts of the spectra are contaminated with night-sky emission lines. There is no significant 35 day modulation present in these spectra.

TABLE 2

HZ HERCULIS ORBITAL PARAMETER SOLUTIONS

$P = 1^{d}.7001677$, $e = 0$

Data[a]	N_{obs}	V_0 (km s^{-1})	K (km s^{-1})	T_0[b] (JD 244+)	σ[c] (km s^{-1})	$\Delta\phi$[d]
Balmer	96	-51 ± 3	52 ± 4	4014.67 ± 0.02	31.3	0.06 ± 0.01
Balmer A	32	-69 ± 4	69 ± 4	4014.75 ± 0.03	17.9	0.11 ± 0.02
Balmer B	37	-39 ± 6	38 ± 8	4014.65 ± 0.07	36.0	0.05 ± 0.04
He I	52	-69 ± 6	42 ± 9	4014.92 ± 0.04	30.8	0.21 ± 0.02
He I A	16	-67 ± 12	31 ± 12	4014.75 ± 0.15	27.4	0.11 ± 0.09
He I B	21	-53 ± 9	33 ± 13	4014.97 ± 0.07	30.5	0.24 ± 0.04
Ca II	66	-56 ± 5	82 ± 7	4014.64 ± 0.02	40.5	0.04 ± 0.01
Ca II A	17	-62 ± 14	80 ± 16	4014.65 ± 0.07	47.5	0.05 ± 0.04
Ca II B	30	-57 ± 7	92 ± 10	4014.63 ± 0.03	37.5	0.03 ± 0.02
Emission	26	...	110 ± 6	4015.10 ± 0.03	48.1	0.31 ± 0.02

[a] $A = \phi_{35d} = 0.25–0.45, 0.75–0.95$; $B = \phi_{35} = 0.0–0.2, 0.5–0.7$.
[b] Time of max positive velocity.
[c] Mean deviation per point of average weight.
[d] Phase shift with respect to exact antiphase with pulsar ($T_0 = 2,441,330.00$).

TABLE 3

35 DAY MODULATION OF ORBITAL VELOCITY $O-C$

Data	N_{obs}	Folding Period (days)	Parameter Tested	Semiamplitude (km s^{-1})	σ (km s^{-1})	ϕ_{35}[a] (max)
Balmer	96	34.928	V_0	10 ± 5	34	0.84
	96	34.928	K	5 ± 5	34	0.93
	96	17.464	V_0	13 ± 5	33	0.33, 0.83
	96	17.464	K	12 ± 5	33	0.36, 0.86
He I	52	34.928	V_0	20 ± 9	35	0.77
	52	17.464	V_0	12 ± 7	36	0.37, 0.87

[a] $2,442,410.349 + 34.928E$.

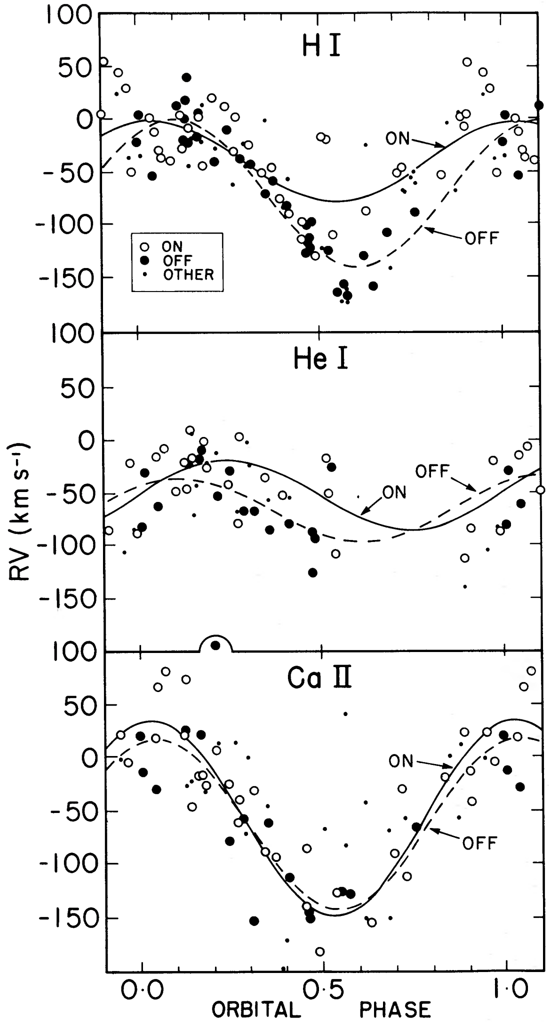

FIG. 2.—Radial velocities of HZ Her plotted on orbital period. ON and OFF refer to the 35 day bins selected, corresponding to high and low heating, respectively. Small symbols are in the intermediate phases. Curves are the circular orbit solutions. Phases indicated are spectroscopic (i.e., X-ray phase + 0.25), so that phase 0.0 is time of primary maximum positive velocity, as determined from the pulsar orbit. Note the phase shifts and different velocity amplitudes. Both H and He I have significantly different "orbits" between the 35 day bins.

2 and Figure 2. We discuss the results in the next section. The line equivalent widths and asymmetries were also divided into the same 35 day cycle bins. Unfortunately, the phase coverage is rather thin when this is done, but there are some points to discuss here too.

Finally, the emission-line velocities were used to derive the orbital parameters shown in Table 2 (and Fig. 2). The errors on these measures are larger, but it is clear that the emission lines are not in phase with the absorption lines, and have larger velocity amplitude. No individual emission-line velocity can be derived from our data since the values are a mean position for all the emission features. The results are similar to (but more significant than) those reported in Paper II.

III. MODELS FOR VELOCITY CURVES

The 17.5 day modulation of the orbital parameters defines the 35 day phases 0.11, 0.61 as having the largest Balmer velocity amplitudes, and 0.36, 0.86 as having the smallest. The V_0 values are smallest at phases 0.08, 0.58, and largest at 0.33, 0.83. The He I results for V_0 are very similar. If the 35 day cycle is understood as a precession of the accretion disk which can occult the central X-ray source, then the optical primary will be most irradiated by its companion at 35 day phases 0.16, 0.66, and most shadowed at phases 0.41 and 0.91. The close coincidence of all these phases suggests that the apparent orbital parameter changes with 35 day cycle may well be principally due to the variable irradiation of the primary. Analysis of the optical light curves (e.g., Howarth and Wilson 1983) has already shown that the stellar continuum is strongly affected by the variable irradiation.

From Tables 2 and 3 it can be seen that the differences between sets of orbital parameters are significant only in the case of the Balmer lines, and for the phasing and V_0 of the He I lines. This may be partly due to the lower accuracy and smaller data sets for the He I and Ca II lines, but we note that these differences (or lack thereof) may also be constraints on models for the star.

In Paper II, we showed how simple models of the heated star can reproduce the general behavior of the three sets of radial velocity and line strength variations (H, He I, Ca II). We have now extended these calculations to examine the effects of variable heating on the primary star. The basic model is a star with a mass ratio 2 Roche lobe surface, with appropriate surface gravity and temperature variations, and a polar temperature of 8500 K. The heated surface is the same as that modeled in Paper II. A "reduced heating" surface was adopted, with a constant temperature of 9500 K. In Figure 3 we show the changes in some measurable quantities between the two models. These changes are very close to the changes detected in our data divided into the chosen 35 day cycle bins. If we apply the appropriate corrections to the derived orbits, for the high and low heating models, we derive six "corrected" orbits whose velocity amplitude values are very close: the mean value for K is 83 ± 3 km s^{-1}. The mean (1.7 day) phase shift of the "corrected" curves is 0.05. While there are thus still deviations from the expected circular orbit, the corrections go a long way toward removing them, including the He I V_0 changes with 35 day phase. Clearly, a more detailed and complex model is required to explain all observed effects, but data of much higher quality would be required to warrant it.

If we accept the criterion that the best model is that which leads to the closest agreement between corrected velocity curves for our three sets of lines, then this model of heating modulation is very satisfactory. There is considerable latitude in the arbitrary, but reasonable heating distributions we can adopt which will yield light and line intensity curves compatible with our observations. However, all of them also give velocity corrections close to the one described. Thus, it appears that we can say with some confidence that the value of the primary star orbital amplitude is well determined at 83 ± 3 km s^{-1}.

The X-ray pulse timing data define the X-ray star velocity very accurately as 169.05 km s^{-1} (Deeter, Boynton, and Pravdo 1981). The X-ray eclipse duration indicates that the inclination of the orbit to the line of sight is within a few degrees of 90. We may therefore determine the stellar masses, with the only significant uncertainty being the optical orbital velocity. The number we give above yields masses of $0.93 \pm 0.07\ M_\odot$ for the pulsar, and 1.91 ± 0.08 for the primary. This result is somewhat different from the values derived by Middleditch and Nelson (1976), although Middleditch (1983)

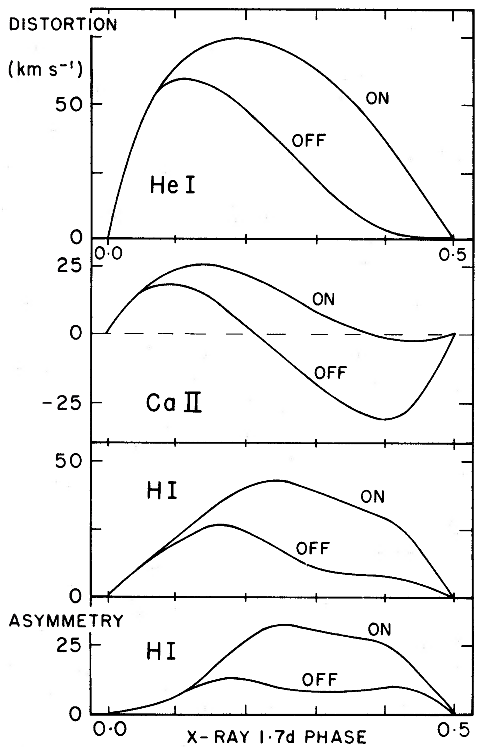

FIG. 3.—Calculated quantities for HZ Her model. *Upper three panels:* deviation of measured line core velocity from star center of mass velocity, for full heating model from Paper II and reduced heating model (OFF) described in text. Line profiles used are similar to those used in Paper II but are not identical, being chosen to match the resolution of the data. *Lower panel:* measure of the Balmer line asymmetry, being the difference between the line centroid and the line core (lower 40%). The sense of all the quantities is reversed between phases 0.5 and 0.0.

suggests that less stringent limits may apply. In either case, the result is model dependent, but our result is perhaps less so, being a more direct estimate of K_{opt}. We also note that all determinations of the mass of Her X-1 yield values lower than those determined for other X-ray pulsars ($\sim 1.6\ M_\odot$). The mass of the whole Her X-1 system is lower than that of the other pulsars studied: this may be a significant evolutionary consideration.

The emission-line velocity variations indicate that they originate principally off-axis, between the stars, as shown in Figure 4. This is close to the surface of the primary star, and at the place deduced by Middleditch and Nelson (1976) and Middleditch (1983) from analysis of the optical pulses. Thus we tend to confirm that the lines are formed in the outer envelope of the primary by X-ray heating, in contrast with the high-mass binaries (Hutchings 1982) in which the emission lines are formed on the accretion disk around the X-ray source. Note that we find that the lines are formed predominantly on the trailing side. This may be in some way connected with the presence of the gas stream between the stars on the leading side (shadowing?). Since the emission is variable and weak, we note that it may arise in several places, and we have only located the mean or strongest part of it. Note that Middleditch (1983) suggests that shadowing may explain some of the emission-line pulsation effects.

IV. SPECTRUM DISCUSSION

Figure 5 shows some line strength and symmetry changes with orbital and 35 day phase. We have used the 35 day phase bins defined by the velocity data, and while the scatter is large, the changes are qualitatively compatible with the variable heating model, although their formal significance is not high. Note that we see no measurable evidence of line emission from the disk, as proposed by Sima (1981). The Balmer and He I line strengths are in general higher in the "heating on" phases, as expected from the simple model. In addition, however, we note the enhancement of Balmer absorption around 1.7 day phase 0.3 and the asymmetry of He I around phase 0.5 in the same sense. There also appears to be a large range of He I line intensity at 1.7 day phases near 0.4. These results suggest an area of enhanced activity or heating on the primary on its trailing side, in the region where the emission lines appear to be strongest. The emission lines themselves appear strongest at both quadratures, although the suggestion is that they peak at opposite quadratures in the high and low heating bins (Fig. 5). This may be different from the 4640 Å emission-line strength as plotted in Paper II, Figure 3, in which case the system may

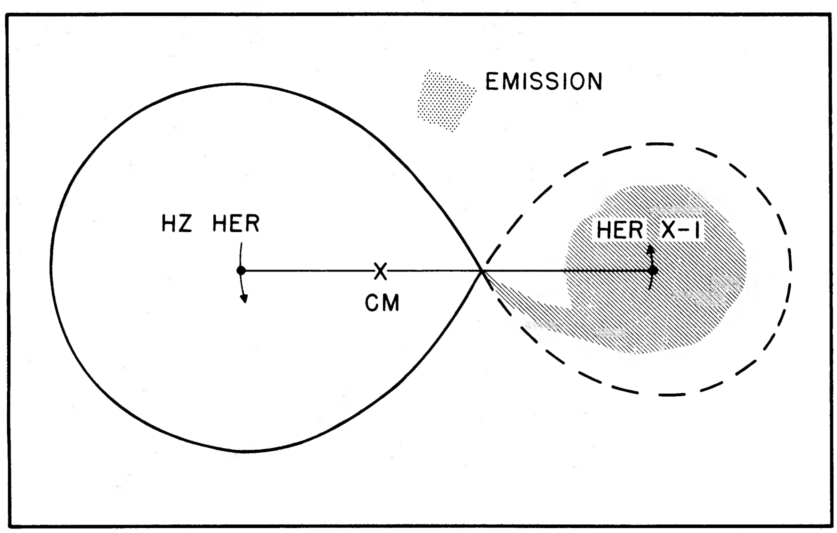

FIG. 4.—Sketch of HZ Her in orbit plane, showing Roche geometry for the mass-ratio derived, and the apparent position of the emission-line region.

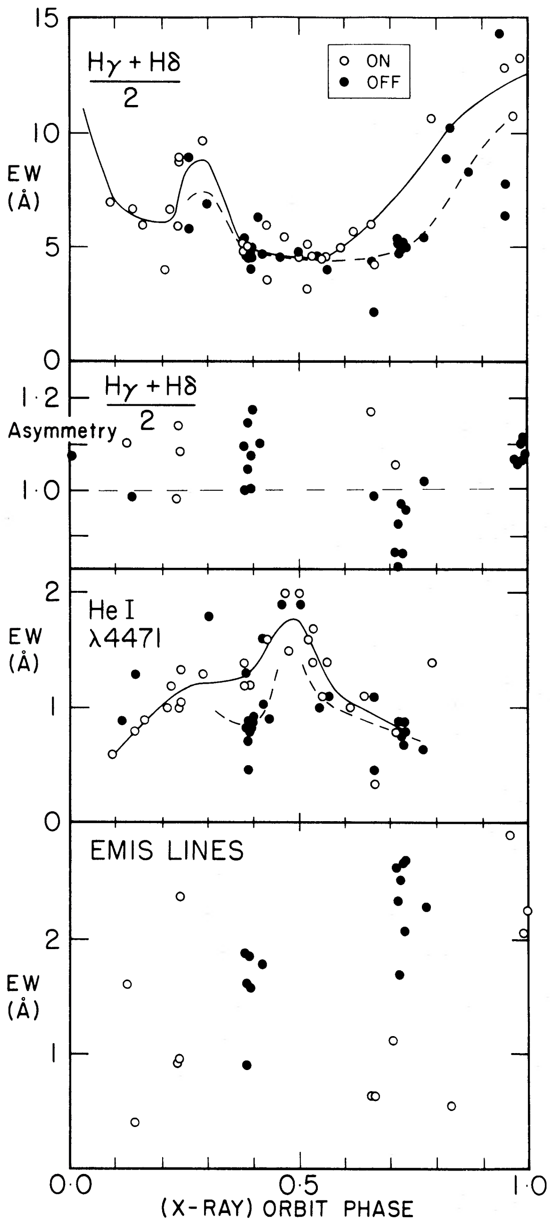

FIG. 5.—Spectral line measures in HZ Her, for the 35 day bins indicated by the radial velocity data. Curves indicate spline fits to the open and closed symbols in the ranges shown. Note the overall difference between ON and OFF bins in H and He I, and also the enhanced line strength in phases 0.3–0.4. The sense of the emission-line intensity variations appears to reverse between the OH and OFF bins.

have undergone a slow change in its structure over the years. Finally, the line asymmetry also seems to differ between the high and low heating 35 day phases, although this indication rests on only two data points. In the low heating phases, the asymmetry changes with 1.7 day phase qualitatively, as expected. If the high heating measures are indicative, the behavior is more complex than the simple model suggests.

We have a few Reticon spectra obtained in 1984. These were not used in the velocity analysis since they are at a lower resolution. However, we note that the spectrum appears normal, and the emission lines (N III and He II) are also normal in equivalent width.

V. SUMMARY

We have found indications that the 35 day cycle of HZ Her shows up in the radial velocities of the primary star. The 35 day phasing of the changes suggests a connection with the expected irradiation of the primary by the X-ray component, with the standard precessing accretion disk model for the system. A simple treatment of the heating modulation leads to corrections to the radial velocity curves which then yield a well-defined orbital velocity amplitude for the primary. This in turn defines the stellar masses in the system. The emission lines are weak and variable, but indicate an overall concentration near to the trailing side of the primary star. The spectrum line strengths of the primary vary in a way generally consistent with the 35 day precession model, although the measures are too sparse to be definitive. There is also indication of enhanced line strength on the primary trailing side, close to the emission line forming region. The apparent phase shift of the absorption line radial velocities, which is present in all data, may also be connected with this asymmetry. The effect was remarked upon in Paper II, and modeled in that paper as a possible tidal lag in the shape of the primary, if its rotation is faster than synchronous. We note also that the optically reprocessed X-ray pulses, as analyzed by Middleditch (1983), also indicate that the pulsed line emission arises on the sides (both of them) of the heated primary. This then is a further point of consistency with our findings.

It is clear that a detailed modeling of the system would require a very large body of data with considerably higher signal-to-noise ratio than ours. It would also require that the system remain in a stable configuration during the time of observation. Thus, the prospects for detailed analysis are not encouraging. It remains of importance to obtain data if and when the system enters an optical and X-ray low state.

We are grateful to Graham Hill for his generous assistance with spectroscopic data reduction problems, and Christopher Morbey for work on his binary orbit programs.

REFERENCES

Bradt, H. V. D., and McClintock, J. E. 1983, *Ann. Rev. Astr. Ap.*, **21**, 13.
Crampton, D. 1974, *Ap. J.*, **187**, 345 (Paper I).
Crampton, D., and Hutchings, J. B. 1974, *Ap. J.*, **191**, 483 (Paper II).
Crosa, L., and Boynton, P. E. 1980, *Ap. J.*, **235**, 999.
Deeter, J. E., Boynton, P. E., and Pravdo, S. H. 1981, *Ap. J.*, **247**, 1003.
Gerend, D., and Boynton, P. E. 1976, *Ap. J.*, **209**, 562.
Gorecki, A., *et al.* 1982, *Ap. J.*, **256**, 234.
Howarth, I. D., and Wilson, B. 1983, *M.N.R.A.S.*, **204**, 1091.
Hill, G., Poeckert, R., and Fischer, W. A. 1982, *Pub. Dom. Astr. Obs. Victoria*, **16**, 43.
Hutchings, J. B. 1982, *Galactic X-Ray Sources*, ed. P. W. Sanford, P. Laskarides, and J. Salton (New York: Wiley), p. 3.
Middleditch, J. 1983, *Ap. J.*, **275**, 278.
Middleditch, J., and Nelson, J. E. 1976, *Ap. J.*, **208**, 567.
Sima, Z. 1982, *Bull. Astr. Inst. Czechoslovakia*, **33**, 122.

D. CRAMPTON, W. A. FISHER, E. M. GIBSON, and J. B. HUTCHINGS: Dominion Astrophysical Observatory, Herzberg Institute of Astrophysics, 5071 W. Saanich Road, Victoria, BC V8X 4M6, Canada